A pressure-stabilized formulation of incompressible flow problems on anisotropic finite element meshes

Jordi Blasco ⋆

Departament de Matemàtica Aplicada I, ETSEIB,
Universitat Politècnica de Catalunya,
Avgda. Diagonal 647,
08038, Barcelona, Spain.

Abstract

We consider a pressure stabilized, finite element approximation of incompressible flow problems in primitive velocity–pressure variables, which is based on a projection of the gradient of the discrete pressure onto the space of discrete functions. Equal order interpolation for the velocity and the pressure can be employed with this formulation. The method introduced here is specially developed to be used on anisotropic finite element meshes with large element aspect ratios.

Key words: Incompressible flows, Stabilized methods, Anisotropic meshes, Navier-Stokes equations

1 Introduction

The numerical approximation of incompressible flow problems presents several difficulties. Apart from the unphysical oscillations in the numerical solution which may appear in convection-dominated flows, the treatment of the incompressibility constrain requires some special attention. The need to enforce the divergence-free condition on the velocity field gives the system a mixed character (see [13]). If standard approximations are employed, such as the Galerkin

⋆ This author's work was partially supported by the Spanish MCYT Project BFM2002-04613-C03-01

Email address: jorge.blasco@upc.es (Jordi Blasco).
URL: http://www-ma1.upc.es/blasco (Jordi Blasco).

finite element method, the discrete spaces for the approximation of the velocity and the pressure are subject to the satisfaction of the well known *inf-sup* condition in order to get stable and convergent solutions. This condition prevents, in particular, the use of the same mesh and the same interpolation for the two variables. Equal interpolation is a very desirable choice not only in terms of ease of implementation but also from a computational viewpoint (see [35]).

Several velocity-pressure finite element pairs have been developed which fulfill the inf-sup condition (see [2], [9] and [12], for instance). Techniques designed to stabilize unstable finite element pairs have also been studied (see [25], [36]). But the most successful methods have been developed under the idea of stabilized formulations, which basically modify the discrete problem in such a way that the inf-sup condition is not required any more. Some examples of pressure-stabilized formulations of incompressible flows are: the Brezzi-Douglas method ([11]), the Douglas-Wang method ([24]), the Galerkin-Least-Squares or GLS method ([26], [27]), first-order least-square methods ([8]), term-by-term stabilization ([15]), (residual-free) bubble function methods ([3], [10]) and unusual stabilized methods ([4]), among several others. Some of these methods are closely related to the treatment of other sources of instability, such as convection.

Another pressure stabilized, finite element formulation of steady, incompressible flows was developed and analyzed in [18], [19] and [22], and extended to the transient case in [7] and [20]. This technique was originally designed under the idea of introducing a projection of the gradient of the discrete pressure onto the space of discrete finite element functions, after which the discrete continuity equation is modified in a consistent way; this is why it was called Pressure-Gradient-Projection method (PGP). Afterwards, it was shown in [17] that in some cases this method can also be obtained within the general framework of subgrid scale models (see [29], [30]), if the so called *orthogonal subscales* approach is followed. Another pressure gradient projection method, based on local projections, was also considered in [6].

On the other hand, most studies of the application of the finite element method to the approximation of two and three dimensional problems, both in fluid mechanics and in other disciplines, rely on the assumption that the finite element meshes satisfy an *aspect ratio* condition, which essentially requires that the elements have a similar size in all the spatial directions. We will call these meshes *isotropic*. However, *anisotropic* meshes with elements having large aspect ratios are often used in many applications, such as the modelling of the hydrodynamics of the ocean in coastal regions if physical coordinates are employed (see [34]), where the horizontal and the vertical length scales may differ by 2 or 3 orders of magnitude. The design of suitable schemes to be used together with anisotropic meshes and their numerical analysis is nowadays an

active subject of research (see [1], [14], [16] and [32], for instance).

In this paper we present a pressure stabilized, finite element formulation of incompressible flow problems which is based on a pressure gradient projection and which is specially developed to be used together with anisotropic meshes. This method is based on the consideration of different elemental stabilization parameters in each of the different spatial directions; these directional elemental stabilization parameters are computed in terms of the element size in each direction, using standard expressions for them. This way, the formulation of well adapted to mesh anisotropy. A similar anisotropically stabilized scheme was analyzed in [5] in the two dimensional, rectangular case using a stabilization technique for the Q_1-Q_1 element. Also, an orthogonal subgrid scale method has been recently introduced in [23] which also emphasizes the use of anisotropic grids; several ways of computing the element sizes in order to obtain the stabilization parameters are compared in that reference, but these parameters are still the same in all directions within each element.

The outline of the paper is as follows: Section 2 introduces the mathematical problem to approximate and some notation. In Section 3 the stabilized, pressure gradient projection method is described, first recalling the isotropic case and then introducing the anisotropic case. Some computational aspects of the discrete problem are discussed in Section 4, whereas in Section 5 numerical results are presented; these results show in particular that the computing times are significantly reduced with the anisotropic scheme compared to the isotropic one on very stretched meshes, and that better accuracy of the solution is also observed with the anisotropic method in some cases.

2 Incompressible flow equations

Let us consider an open, bounded domain $\Omega \subset \mathbb{R}^d$, with $d = 2$ or 3, which we assume to be polygonal or polyhedral. The boundary of Ω is denoted by Γ. If the region Ω is occupied by a Newtonian incompressible fluid in motion at a steady state, the velocity $\mathbf{u}$ and the pressure p of the fluid at each point of Ω satisfy the incompressible Navier-Stokes equations:

$$(\mathbf{u} \cdot \nabla)\mathbf{u} - \nu \Delta \mathbf{u} + \nabla p = \mathbf{f} \text{ in } \Omega \tag{1}$$

$$\nabla \cdot \mathbf{u} = 0 \text{ in } \Omega \tag{2}$$

$$\mathbf{u} = \mathbf{0} \text{ on } \Gamma \tag{3}$$

Here, and in what follows, boldface characters denote vector quantities. In the momentum equation (1), ∇ and Δ are the gradient and Laplacian operators, respectively, $\nu > 0$ is the fluid's kinematic viscosity (which we assume constant), and $\mathbf{f}$ is a given forcing term. In the continuity equation (2), $\nabla \cdot \mathbf{u}$ is

the divergence of the velocity field; this equation, therefore, enforces incompressibility. Finally, we have assumed the homogeneous Dirichlet boundary condition (3) for simplicity.

In order to study problem (1)-(2)-(3), the following Hilbert spaces are usually considered: $L^2(\Omega)$ denotes the space of square integrable functions on Ω, with scalar product (u, v) and norm $\|u\|$; $H^m(\Omega)$ is the space of functions of $L^2(\Omega)$ with distributional derivatives up to order m also belonging to $L^2(\Omega)$; $H_0^1(\Omega)$ is the closed subspace of $H^1(\Omega)$ of functions that vanish on Γ, a space on which $\|\nabla u\|$ is a norm equivalent to that induced by $H^1(\Omega)$; $H^{-1}(\Omega)$ is the dual space of $H_0^1(\Omega)$, the duality between the two been denoted by $<,>$. The corresponding vector (product) spaces are likewise denoted by boldface characters in all cases.

Assuming that $\mathbf{f} \in \mathbf{H}^{-1}(\Omega)$, the weak form of problem (1)-(2)-(3) consists in finding $\mathbf{u} \in V := \mathbf{H}_0^1(\Omega)$ and $p \in Q := L_0^2(\Omega)$ (the space of functions of $L^2(\Omega)$ with zero mean on Ω) such that:

$$((\mathbf{u} \cdot \nabla)\mathbf{u}, \mathbf{v}) \; + \; \nu(\nabla \mathbf{u}, \nabla \mathbf{v}) \; - \; (p, \nabla \cdot \mathbf{v}) =< \mathbf{f}, \mathbf{v} >, \forall \mathbf{v} \in V \qquad (4)$$

$$(\nabla \cdot \mathbf{u}, q) = \; 0, \qquad \forall q \in Q \qquad (5)$$

If the domain Ω is Lipschitz continuous, problem (4)-(5) has at least one solution (see, for instance, [28]), which is unique under certain conditions (in particular, for sufficiently large ν). If Ω is smooth enough, or if it is a bounded convex polygon, and $\mathbf{f} \in \mathbf{L}^2(\Omega)$, then the solution has the additional regularity $\mathbf{u} \in \mathbf{H}^2(\Omega)$ and $p \in H^1(\Omega)$ (see [28]); we assume the latter regularity for the pressure from now on.

3 Numerical approximation

3.1 Isotropic stabilized method

We recall here the stabilized, pressure-gradient-projection formulation analyzed in [19]. Let Θ_h be a partition of Ω (of size $h > 0$) into finite elements $K \in \Theta_h$; we assume that each element K is the image of a reference element $\hat{K}$ by an affine mapping $F_K \colon \hat{K} \to K$. We consider the following spaces of discrete functions for the numerical approximation of problem (4)-(5):

$$Q_h = \left\{ q_h \in \mathcal{C}^0(\Omega) \,/\, \forall\, K \in \Theta_h,\, q_{h|K} = \hat{q}_h \circ F_K^{-1},\, \hat{q}_h \in R_{k_p}(\hat{K}) \right\}$$

$$V_h = \left\{ \mathbf{v}_h \in (\mathcal{C}^0(\Omega))^d \,/\, \forall\, K \in \Theta_h,\, \mathbf{v}_{h|K} = \hat{\mathbf{v}}_h \circ F_K^{-1},\, \hat{\mathbf{v}}_h \in (R_{k_u}(\hat{K}))^d \right\}$$

$$V_{h,0} = \left\{ \mathbf{v}_h \in V_h \,/\, \mathbf{v}_{h|\Gamma} = \mathbf{0} \right\}$$

where $R_k(D)$ is the polynomial space of degree k on D, if $\hat{K}$ is a simplex, or the space of polynomials of degree less than or equal to k in each variable, if $\hat{K}$ is a square or a cube. Q_h is the space of discrete pressures and $V_{h,0}$ is the space of discrete velocities, whereas V_h will be the space of the projection of the pressure gradient. Given now a set of elemental parameters $\{\alpha_K\}_{K\in\Theta_h}$ such that $\alpha_K > 0 \quad \forall K \in \Theta_h$, to be determined later on, we consider the following stabilized method, where for each element K we denote by $(u,v)_K$ the scalar product in $L^2(K)$:

Find $(\mathbf{u}_h, p_h, \mathbf{r}_h) \in V_{h,0} \times Q_h \times V_h$ such that, for all $(\mathbf{v}_h, q_h, \mathbf{s}_h) \in V_{h,0} \times Q_h \times V_h$:

$$((\mathbf{u}_h \cdot \nabla)\mathbf{u}_h, \mathbf{v}_h) \; + \; \nu(\nabla \mathbf{u}_h, \nabla \mathbf{v}_h) \; - \; (p_h, \nabla \cdot \mathbf{v}_h) = < \mathbf{f}, \mathbf{v}_h > \tag{6}$$

$$(\nabla \cdot \mathbf{u}_h, q_h) + \sum_{K\in\Theta_h} (\alpha_K \nabla p_h \; - \; \sqrt{\alpha_K}\, \mathbf{r}_h, \nabla q_h)_K = 0 \tag{7}$$

$$(\mathbf{r}_h, \mathbf{s}_h) \; - \; \sum_{K\in\Theta_h} \sqrt{\alpha_K}\, (\nabla p_h, \mathbf{s}_h)_K = 0 \tag{8}$$

It is clear from (8) that $\mathbf{r}_h$ is the orthogonal projection in the space $\mathbf{L}^2(\Omega)$ of the gradient of the discrete pressure (∇p_h), scaled within each element by $\sqrt{\alpha_K}$, onto the space of discrete vector functions V_h. This method was proved in [19] to yield stable and optimally convergent solutions, provided the approximating spaces $V_{h,0}$ and Q_h satisfy a mild compatibility condition, which was proved to hold for most equal order interpolations ($k_u = k_p$).

The determination of the stabilization coefficients α_K is one of the key issues in the development of stabilized methods. The numerical analysis of the convergence of the scheme (6)-(7)-(8) requires that there exist two positive constants α_0 and α_1 such that, for all $K \in \Theta_h$:

$$\alpha_0 h_K^2 \; \leq \; \alpha_K \; \leq \; \alpha_1 h_K^2$$

where h_K is the size of element K. We therefore compute these parameters by the simple expression:

$$\alpha_K = \bar{\alpha}\, \frac{h_K^2}{\nu}, \;\; \forall K \in \Theta_h$$

where $\bar{\alpha}$ is a fixed constant; however, more general formulations will also be considered later on.

3.2 Anisotropic stabilized method

The stabilization coefficients α_K of the method just described depend on the overall element size h_K, irrespective of the element geometry. In several applications, very stretched meshes are often used, with very different element

sizes in the different space directions. In those cases, it would seem more appropriate to consider different stabilization parameters within each element in each direction. Thus, we now consider the following anisotropically stabilized scheme:

Find $(\mathbf{u}_h, p_h, \mathbf{r}_h) \in V_{h,0} \times Q_h \times V_h$ such that, for all $(\mathbf{v}_h, q_h, \mathbf{s}_h) \in V_{h,0} \times Q_h \times V_h$:

$$((\mathbf{u}_h \cdot \nabla)\mathbf{u}_h, \mathbf{v}_h) \; + \; \nu(\nabla \mathbf{u}_h, \nabla \mathbf{v}_h) - (p_h, \nabla \cdot \mathbf{v}_h) = < \mathbf{f}, \mathbf{v}_h > \tag{9}$$

$$(\nabla \cdot \mathbf{u}_h, q_h) + \sum_{K \in \Theta_h} \sum_{i=1,\ldots,d} (\alpha_{K,i} \partial_i p_h - \sqrt{\alpha_{K,i}} r_{h,i}, \partial_i q_h)_K = 0 \tag{10}$$

$$(\mathbf{r}_h, \mathbf{s}_h) - \sum_{K \in \Theta_h} \sum_{i=1,\ldots,d} \sqrt{\alpha_{K,i}} \, (\partial_i p_h, s_{h,i})_K = 0 \tag{11}$$

where $\mathbf{r}_h = (r_{h,1}, \ldots, r_{h,d})$, $\mathbf{s}_h = (s_{h,1}, \ldots, s_{h,d})$ and now

$$\alpha_{K,i} \; = \; \bar{\alpha} \, \frac{h_{K,i}^2}{\nu}, \;\; \forall i = 1, \ldots, d, \;\; \forall K \in \Theta_h$$

Here, $h_{K,i}$ is the size of element K in the i-th direction (which we compute as the maximum absolute value of the difference between the i-th coordinates of pairs of nodes in K).

4 Computational aspects

Both the isotropic ((6)-(7)-(8)) and the anisotropic ((9)-(10)-(11)) PGP methods can be written in matrix form as follows:

$$K(U)U \; + \; GP \qquad\quad = F_u \tag{12}$$

$$DU \; + \; L_\alpha P \; - \; D_\alpha R = F_p \tag{13}$$

$$-G_\alpha P \; + \; MR = 0 \tag{14}$$

where:

- U, P and R represent the vectors of nodal values of velocity (without its prescribed values), pressure and pressure-gradient-projection, respectively.
- $K(U)$ is the stiffness matrix, accounting for convection and diffusion.
- G and D are the gradient and divergence matrices, respectively, where the rows (respectively, columns) associated to prescribed velocity values have been omitted.
- L_α, D_α and G_α are the pressure Laplacian, PGP divergence and pressure gradient matrices, respectively, which take into account the effect of the

weighting in each element with the stability coefficients α_K ($\alpha_{K,i}$, in the anisotropic case).
- M is the mass matrix.
- F_u and F_p are known vectors arising from the RHS term $\mathbf{f}$ in (1) and eventually from inhomogeneous boundary conditions.

In Reference [22], a detailed comparison of several iterative schemes designed to solve the nonlinear, coupled problem (12)-(13)-(14) was given; the most efficient method proved to be a pair of nested loops consisting of an outer iteration to account for the nonlinearity of the problem and an inner iteration segregating the computation of the velocity and the pressure from that of the pressure gradient projection. Namely, given an initial approximation U^0 to the velocity solution, an iterative method is considered to solve the nonlinearity of the problem; here, we employ a Picard method, although other schemes (such as Newton-Raphson's) were also tested. Thus, for each $j \geq 1$, we have to compute (U_j, P_j, R_j) such that:

$$\begin{aligned} K(U_{j-1})U_j \;+\; GP_j \qquad\qquad &= F_u && (15)\\ DU_j \;+\; L_\alpha P_j \;-\; D_\alpha R_j &= F_p && (16)\\ -\,G_\alpha P_j \;+\; MR_j &= 0 && (17) \end{aligned}$$

Then, in order to solve the linear problem (15)-(16)-(17) for each j, we take $R_j^0 = R_{j-1}$ and obtain each new iterate (U_j^i, P_j^i, R_j^i), for $i \geq 1$, by calculating the velocity and the pressure assuming a known value of the PGP, which is then updated at the end of the iteration, in a *block-Gauss-Seidel* way:

$$\begin{aligned} K(U_{j-1})U_j^i \;+\; GP_j^i &= F_u && (18)\\ DU_j^i \;+\; L_\alpha P_j^i &= F_p \;+\; D_\alpha R_j^{i-1} && (19)\\ MR_j^i &= G_\alpha P_j^i && (20) \end{aligned}$$

This way, the system matrix for the velocity-pressure problem is unaltered through the inner iteration process (and thus it only needs to be computed once every outer iteration) and the system matrix for the PGP problem is the mass matrix (which can be *lumped* leading to a diagonal system).

5 Numerical test cases

We present in this Section some numerical results obtained with the anisotropic, PGP stabilized method (9)-(10)-(11) on some standard test cases; we include

also the results obtained with the isotropic scheme (6)-(7)-(8) for comparison purposes.

5.1 Kovasznay flow

We first consider a problem introduced by Kovasznay (see [31]), modelling laminar flow behind a two dimensional grid, in which an analytical solution of the two-dimensional, steady, incompressible Navier-Stokes equations (1)-(2) with no forcing term is available. The velocity solution $\mathbf{u} = (u, v)$ is given by:

$$u(x,y) = 1 - e^{\lambda x}\cos(2\pi y) \tag{21}$$

$$v(x,y) = \frac{\lambda}{2\pi} e^{\lambda x}\sin(2\pi y) \tag{22}$$

for $(x, y) \in \mathbb{R}^2$, whereas the pressure is:

$$p(x,y) = p_0 - \frac{1}{2}e^{2\lambda x} \tag{23}$$

where p_0 is an arbitrary constant and the parameter λ is given in terms of the Reynolds Re number by:

$$\lambda = \frac{\mathrm{Re}}{2} - (\frac{\mathrm{Re}^2}{4} + 4\pi^2)^{1/2} < 0$$

We solved this flow problem in the domain $\Omega = [-\frac{1}{2}, 1] \times [-\frac{1}{2}, \frac{1}{2}]$ for a value of the Reynolds number equal to 40, prescribing the velocity values of the exact solution (21)-(22) on the boundary of Ω. This problem was also solved in [22], where the isotropic PGP method was used on four uniform meshes and with four different types of elements of first and second order on each mesh; a comparison with the GLS method (equivalent in this case to an Algebraic Subgrid Scale approach) showed that the PGP method gives more accurate results for the pressure solution than the GLS method if first order elements are used, the velocity errors being the same for the two schemes. However, both in this and in other test cases solved it was found that the PGP formulation requires about 20% more computational time that the GLS method to reach convergence.

In order to compare the performance of the isotropic and the anisotropic versions of the PGP stabilized formulation, we solved this problem on four meshes of bilinear quadrilateral elements (Q_1) made up from 20 uniform subdivisions in the y variable and 60, 300, 1500 and 3000 uniform subdivisions in the x

Mesh	Aspect ratio	$\|\|\mathbf{u}-\mathbf{u}_h\|\|$	$\|\|p-p_h\|\|$	$\|\|\nabla(\mathbf{u}-\mathbf{u}_h)\|\|$	$\|\|\nabla(p-p_h)\|\|$
60×20	2	I: $7.7 \cdot 10^{-3}$	$1.0 \cdot 10^{-2}$	$4.6 \cdot 10^{-1}$	$2.7 \cdot 10^{-2}$
		A: $7.7 \cdot 10^{-3}$	$9.9 \cdot 10^{-3}$	$4.6 \cdot 10^{-1}$	$2.7 \cdot 10^{-2}$
300×20	10	I: $7.7 \cdot 10^{-3}$	$1.1 \cdot 10^{-2}$	$4.6 \cdot 10^{-1}$	$2.0 \cdot 10^{-2}$
		A: $7.7 \cdot 10^{-3}$	$1.0 \cdot 10^{-2}$	$4.6 \cdot 10^{-1}$	$2.0 \cdot 10^{-2}$
1500×20	50	I: $7.7 \cdot 10^{-3}$	$1.1 \cdot 10^{-2}$	$4.6 \cdot 10^{-1}$	$2.0 \cdot 10^{-2}$
		A: $7.7 \cdot 10^{-3}$	$1.1 \cdot 10^{-2}$	$4.6 \cdot 10^{-1}$	$2.3 \cdot 10^{-2}$
3000×20	100	I: $7.7 \cdot 10^{-3}$	$1.0 \cdot 10^{-2}$	$4.6 \cdot 10^{-1}$	$2.2 \cdot 10^{-2}$
		A: $7.7 \cdot 10^{-3}$	$1.1 \cdot 10^{-2}$	$4.6 \cdot 10^{-1}$	$5.1 \cdot 10^{-2}$

Table 1
Kovasznay flow: aspect ratio and errors on four increasingly stretched meshes.

Mesh	Isotropic	Anisotropic	Anisotr./Isotr.
60×20	3.36	2.76	82%
300×20	31.47	16.22	51%
1500×20	291.79	79.21	27%
3000×20	713.88	156.56	22%

Table 2
Kovasznay flow: CPU time (in seconds) for convergence on each mesh for the isotropic and the anisotropic schemes, and percentage of the latter to the former.

variable, respectively; the four meshes are, thus, increasingly stretched. A tolerance value of 10^{-3} in the relative error of the velocity, the pressure and the pressure gradient projection was set for the convergence of the nonlinearity in all cases, while a value of 10^{-4} was used for the tolerance of the inner, PGP iterations. In this numerical example, the method of nested iterations (18)-(19)-(20) was used to solve the discrete problems (6)-(7)-(8) and (9)-(10)-(11), with a direct method for the solution of the linear systems of equations for the velocity and the pressure and a consistent mass matrix for the pressure gradient projection. All the computations were performed on a PC with a AMD processor at 1.2 Gh.

The aspect ratio of the elements of each mesh is given in Table (1), together with the errors with respect to the exact solution (21)-(22)-(23) for both the velocity and the pressure, in the norms of $L^2(\Omega)$ and $H^1(\Omega)$ and for both the isotropic (I) and the anisotropic (A) methods. Very similar accuracy is achieved with the two schemes in all cases, the error being governed by the (relatively large) vertical spacing.

Mesh	Iter. 1	Iter. 2	Iter. 3	Iter. 4	Iter. 5	Iter. 6	Iter. 7
60×20	I: 35	41	24	14	8	3	2
	A: 33	20	20	12	6	3	2
300×20	I: 97	75	52	25	6	3	2
	A: 36	32	21	12	5	2	2
1500×20	I: 245	153	78	18	6	3	2
	A: 34	30	18	11	5	2	2
3000×20	I: 303	210	75	19	6	3	2
	A: 32	28	18	11	5	2	2

Table 3
Kovasznay flow: number of inner iterations for each outer iterarion.

The overall CPU time required for convergence with the two schemes on each mesh, and the percentage of that of the anisotropic method with respect to that of the isotropic one, are given in Table (2). A smaller computational time for the anisotropic method is observed in all cases, it being as low as 22% that of the isotropic one on the most stretched mesh. The reason for this decrease of CPU time with the anisotropic method is understood if one looks at the number of outer and inner iterations performed in each case, which is given in Table (3). While the number of outer, nonlinear iterations is always the same for the two schemes (7), the number of inner iterations within each outer iteration is much lower in the anisotropic case. Since these inner iterations can be understood as a block-Gauss-Seidel method, this decrease can be ultimately related to a smaller condition number of the overall system matrix for the (linearized) velocity-pressure-pressure gradient problem in the anisotropic case.

5.2 3D Cavity flow problem

As a second example, we solved the lid-driven, cubic cavity flow problem. The domain is the unit cube $\Omega = [0,1]^3$ and the velocity is set to zero on all the boundary except for the top lid $y = 1$, which moves with a constant velocity $\mathbf{u} = (1,0,0)$ (see Figure 1). One nodal pressure is also set to zero to avoid the constant mode. We used a cartesian mesh with 4480 trilinear hexahedral elements and 5355 nodal points, which is refined near all the boundaries; the direction of element stretching changes throughout the mesh, thus making the use of anisotropic techniques convenient in this example.

In this case, we used a time-stepping method in order to obtain the solution as a steady state. The time advancement is based on a backward Euler method,

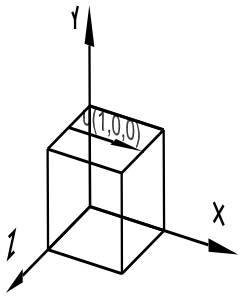

Fig. 1. Cubic cavity flow problem: geometry and boundary conditions.

which is unconditionally stable, in which all the terms are treated implicitly (but for the convective term, which is linearized). Given a time step size $\delta t > 0$, the solution at $t_{n+1} = (n+1)\delta t$ is obtained as:

$$\frac{1}{\delta t}(\mathbf{u}^{n+1} - \mathbf{u}^n) \; + \; (\mathbf{u}^n \cdot \nabla)\mathbf{u}^{n+1} \; - \; \nu\Delta\mathbf{u}^{n+1} \; + \; \nabla p^{n+1} = \mathbf{f} \;\; \text{in} \;\; \Omega$$
$$\nabla \cdot \mathbf{u}^{n+1} = 0 \;\; \text{in} \;\; \Omega$$

A Pressure-Gradient-Projection stabilization technique is applied in each time step, so that the discrete problem reads:

Find $(\mathbf{u}_h^{n+1}, p_h^{n+1}, \mathbf{r}_h^{n+1}) \in V_{h,0} \times Q_h \times V_h$ such that, for all $(\mathbf{v}_h, q_h, \mathbf{s}_h) \in V_{h,0} \times Q_h \times V_h$:

$$\frac{1}{\delta t}(\mathbf{u}_h^{n+1} - \mathbf{u}_h^n, \mathbf{v}_h) + ((\mathbf{u}_h^n \cdot \nabla)\mathbf{u}_h^{n+1}, \mathbf{v}_h) + \nu(\nabla\mathbf{u}_h^{n+1}, \nabla\mathbf{v}_h)$$
$$-(p_h^{n+1}, \nabla \cdot \mathbf{v}_h) \; = < \mathbf{f}, \mathbf{v}_h > \qquad (24)$$
$$(\nabla \cdot \mathbf{u}_h^{n+1}, q_h) + \sum_{K \in \Theta_h} \sum_{i=1,\ldots,d} (\alpha_{K,i}\partial_i p_h^{n+1} - \sqrt{\alpha_{K,i}} r_{h,i}^{n+1}, \partial_i q_h)_K = 0 \qquad (25)$$
$$(\mathbf{r}_h^{n+1}, \mathbf{s}_h) - \sum_{K \in \Theta_h} \sum_{i=1,\ldots,d} \sqrt{\alpha_{K,i}} \, (\partial_i p_h^{n+1}, s_{h,i})_K = 0 \qquad (26)$$

This discrete problem was also solved in an iterative way by a block-Gauss-Seidel type method similar to (18)-(19)-(20), in which the computation of the velocity and the pressure is split from that of the pressure gradient projection.

The stabilization coefficients $\alpha_{K,i}$ were now computed using the following general expression, which is frequently used in the GLS method (see [27] for further discussion on the choice of the stabilizing parameters and [21] for a derivation of the isotropic equivalent of the following expression from a Fourier analysis):

$$\alpha_{K,i} \;=\; \Big(c_1 \frac{\nu}{h_{K,i}^2} \;+\; c_2 \frac{v_{K,i}}{h_{K,i}} \;+\; \frac{1}{\delta t}\Big)^{-1}, \;\; i = 1, 2, 3$$

where $v_{K,i}$ is a characteristic value of the i-th component of the velocity on element K and c_1, c_2 are algorithmic parameters, adequate values for which are generally agreed to be $c_1 = 12$ and $c_2 = 2$ for linear elements (see [27]).

We solved the cubic cavity flow problem for a value of the Reynolds number equal to 400, for which a steady solution is known to exist. Starting from the fluid at rest, we performed the time stepping scheme (24)-(25)-(26) with $\delta t = 0.03$ until a steady state was reached, with a tolerance value of $\epsilon_s = 10^{-5}$. Within each time step, convergence of the PGP uncoupling was checked with a tolerance of $\epsilon_g = 10^{-6}$. During the first 10 time steps of the computation, we solved the linear systems for the velocity and the pressure with a direct LDU method and those for the pressure gradient projection with a consistent mass matrix and also a direct solution method. In the following time steps, when an initial guess could be taken close enough to the solution to ensure convergence, an iterative BiCStab method with left ILUT preconditioning was employed for the velocity-pressure systems, while a lumped mass matrix was used for the pressure gradient systems.

In order to test the performance of the anisotropic stabilization technique, we also solved this problem with the isotropic scheme equivalent to (24)-(25)-(26). It took 693 steps to reach a steady state with the isotropic method (which took about 52 minutes of CPU) while 686 steps (and about 42 minutes) were needed with the anisotropic scheme; a fixed number of 2 PGP iterations were required in all time steps of both methods.

The flow pattern and the pressure contours in the mid-planes $x = 0.5$, $y = 0.5$ and $z = 0.5$ obtained with the anisotropic scheme (24)-(25)-(26) can be seen in Figures 2 and 3, respectively. These results are in good agreement with those obtained in [33], where a least-square finite element method was used on a velocity-pressure-vorticity formulation with a mesh of 65000 trilinear elements on half of the domain.

Figure 4 displays the profiles of the u-velocity component along the vertical centerline $\{x = 0.5, z = 0.5\}$; the results of [33] are also plotted for comparison. A better fitting is observed for the anisotropic method. In order to quantify the accuracy of our solutions, we computed the Euclidean norm of the error in the nodal u-velocity vector along this centerline with respect to the reference solution of [33]; due to differences in the y-variable of the layers of elements between the mesh used in [33] and ours, we interpolated the reference solution to our nodes. The errors thus obtained were 0.3976 for the isotropic scheme and 0.0779 for the anisotropic one.

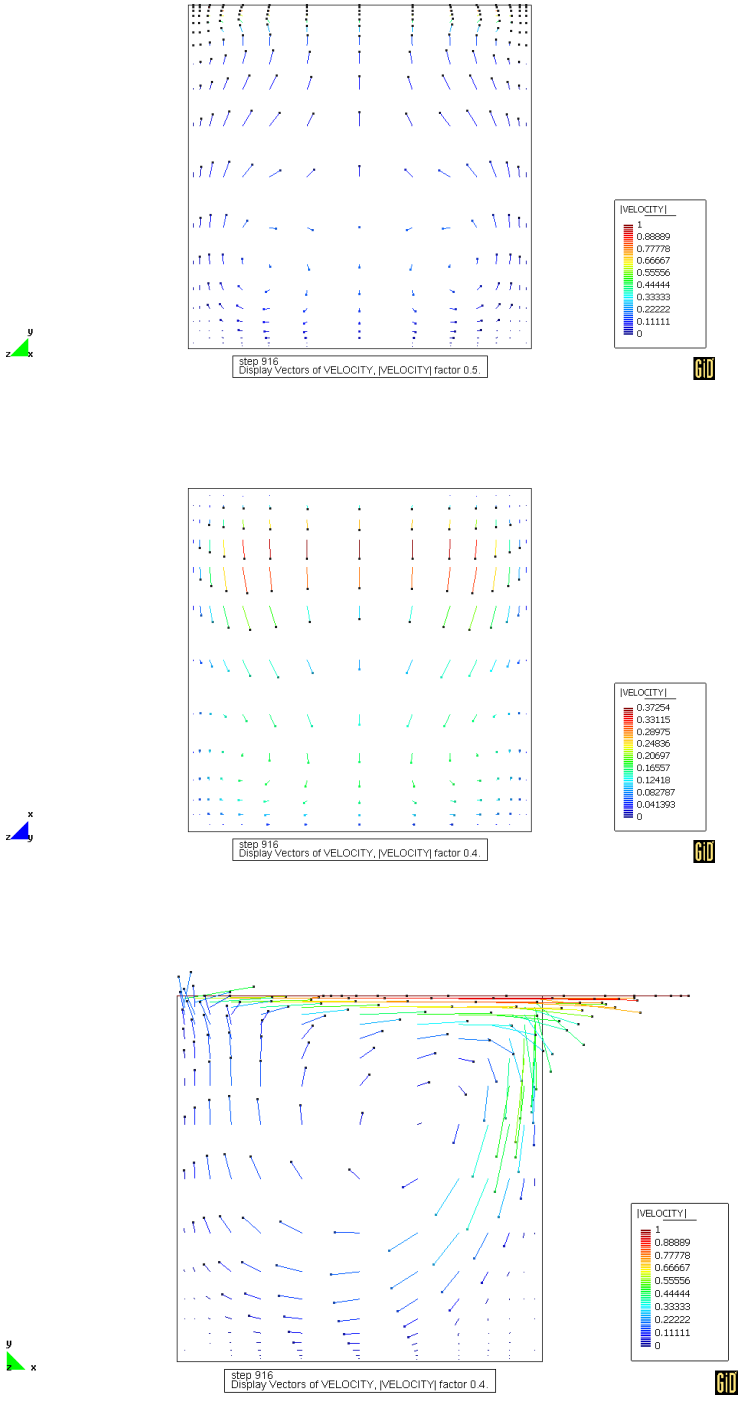

Fig. 2. Flow pattern at the mid-planes $x = 0.5$ (top), $y = 0.5$ (center) and $z = 0.5$ (bottom).

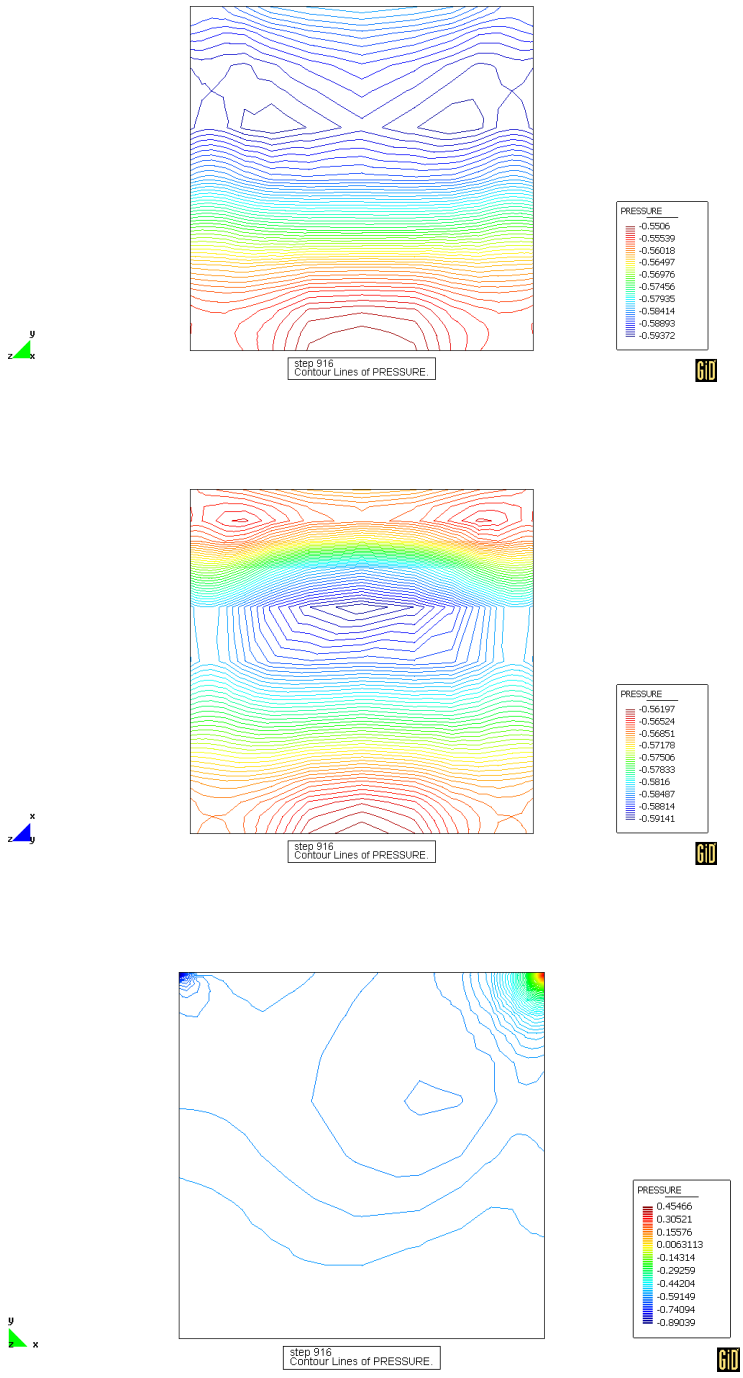

Fig. 3. Pressure contours at the mid-planes $x = 0.5$ (top), $y = 0.5$ (center) and $z = 0.5$ (bottom).

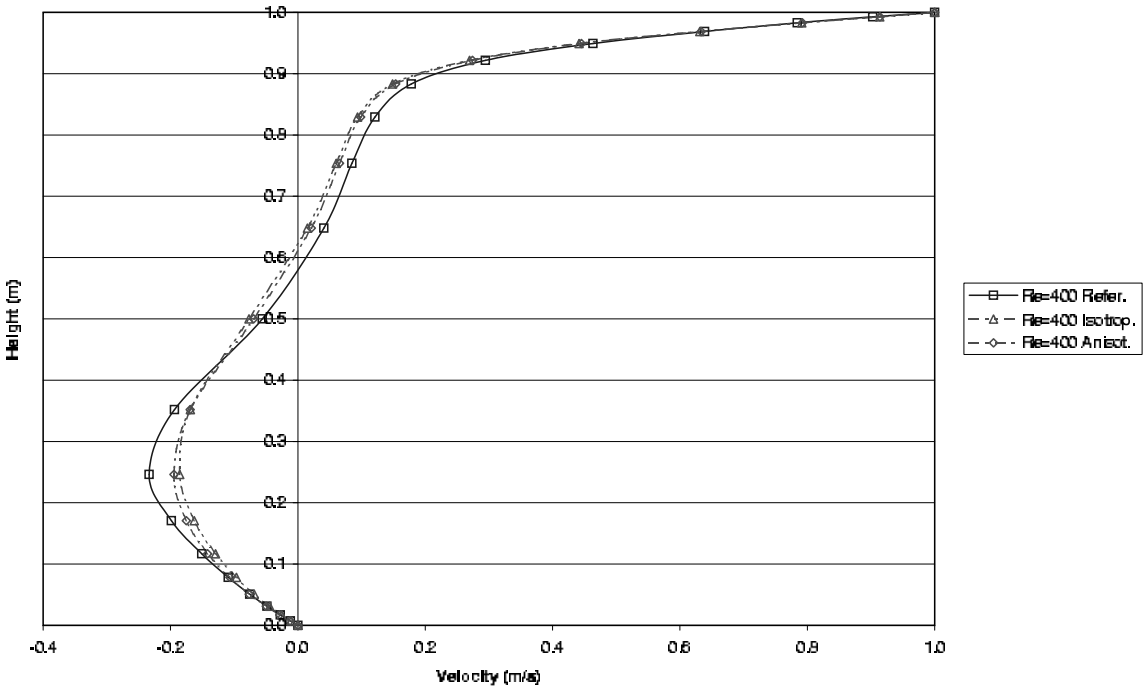

Fig. 4. u-velocity component along the centerline $x = 0.5, z = 0.5$.

6 Conclusions

An anisotropic, pressure stabilization technique for incompressible flow problems has been developed and applied to standard test cases in two and three dimensions, showing better numerical performance than its isotropic equivalent on very stretched finite element meshes (with aspect ratios of order 1/100). The use of anisotropic methods seems also convenient on more regular meshes. The numerical analysis of anisotropic techniques, however, is still an open problem.

References

[1] T. Apel and G. Lube, Anisotropic mesh refinement in stabilized Galerkin methods, Numer. Math. 74 (1996) 261-282.

[2] D.N. Arnold, F. Brezzi and M. Fortin, A stable finite element for the Stokes equations, Calcolo 21 (1984) 337-344.

[3] C. Baiocci, F. Brezzi and L.P. Franca, Virtual bubbles and Galerkin–least–squares type methods (Ga.L.S.), Comp. Meth. Appl. Mech. Eng. 105 (1993) 125-141.

[4] G. Barrenechea and F. Valentin, An unusual stabilized finite element method for a generalized Stokes problem, Numer. Math. 92 (2002) 635-677.

[5] R. Becker and R. Rannacher, Finite element solution of the incompressible Navier-Stokes equations on anisotropically refined meshes, Notes Numer. Fluid Mech. 49 (1995).

[6] R. Becker and M. Braack, A finite element pressure gradient stabilization for the Stokes equations based on local projections, Calcolo 38 (2001) 173-199.

[7] J. Blasco and R. Codina, Space and time error estimates for a first order, pressure stabilized finite element method for the incompressible Navier-Stokes equations, Applied Numer. Math. 38 (2001) 475-497.

[8] P. Bochev, Z. Cai, T.A. Manteuffel and S.F. McCormick, Analysis of velocity-flux first-order system least-square principles for the Navier-Stokes equations. I, SIAM Jour. Numer. Anal. 35 (1998) 990-1009.

[9] D. Boffi, Three-dimensional finite element methods for the Stokes problem, SIAM Jour. Numer. Anal. 34 (1997) 664-670.

[10] F. Brezzi, M.O. Bristeau, L.P. Franca, M. Mallet and G. Rogé, A relationship between stabilized finite element methods and the Galerkin method with bubble functions, Comp. Meth. Appl. Mech. Eng. 96 (1992) 117-129.

[11] F. Brezzi and J. Douglas, Stabilized mixed methods for the Stokes problem, Numer. Math. 53 (1988) 225-235.

[12] F. Brezzi and R.S. Falk, Stability of higher–order Hood–Taylor methods, SIAM Jour. Numer. Anal. 28 (1991) 581-590.

[13] F. Brezzi and M. Fortin, Mixed and Hybrid finite element methods, (Springer Series in Computational Mathematics, 15. Springer–Verlag, 1991).

[14] C. Canuto and A. Tabacco, An anisotropic functional setting for convection diffusion problems, East-West Jour. Numer. Math. 9 (2001) 199-231.

[15] T. Chacón, A term-by-term stabilization algorithm for the finite element solution of incompressible flow problems, Numer. Math. 79 (1998) 283-319.

[16] S. Chen, Y. Zhao and D. Shi, Anisotropic interpolations with application to nonconforming elements, Applied Numer. Math. 49 (2004) 135-152.

[17] R. Codina, Stabilization of incompressibility and convection through orthogonal subscales in finite element methods, Comp. Meth. Appl. Mech. Eng. 190 (2000) 1579-1599.

[18] R. Codina and J. Blasco, A finite element formulation for the Stokes problem allowing equal velocity-pressure interpolation, Comp. Meth. Appl. Mech. Eng. 143, 3-4 (1997) 373-391.

[19] R. Codina and J. Blasco, Analysis of a pressure–stabilized finite element approximation of the stationary Navier-Stokes equations, Numer. Math. 87 (2000) 59-81.

[20] R. Codina and J. Blasco, Stabilized finite element method for the transient Navier-Stokes equations based on a pressure gradient projection, Comp. Meth. Appl. Mech. Eng. 182, 3-4 (2000) 277-300.

[21] R. Codina and J. Blasco, Analysis of a stabilized finite element approximation of the transient convection-diffusion-reaction equation using orthogonal subscales, Comput. Visual. Sci. 4 (2002) 167-174.

[22] R. Codina, J. Blasco, G.C. Buscaglia and A. Huerta, Implementation of a stabilized finite element formulation for the incompressible Navier-Stokes equations based on a pressure gradient projection, Int. Jour. Numer. Meth. Fluids 37 (2001) 419-444.

[23] R. Codina and O. Soto, Approximation of the incompressible Navier-Stokes equations using orthogonal subscale stabilization and pressure segregation on anisotropic meshes, Comp. Meth. Appl. Mech. Eng. 193 (2004), 1403-1419.

[24] J. Douglas and J. Wang, An absolutely stabilized finite element method for the Stokes problem, Math. Comp. 52 (1989) 495-508.

[25] M. Fortin and S. Boivin, Iterative stabilization of the bilinear-velocity, constant-pressure element, Int. Jour. Numer. Meth. Fluids 10 (1990) 125-140.

[26] L.P. Franca and S.L. Frey, Stabilized finite element methods: II. The incompressible Navier-Stokes equations, Comp. Meth. Appl. Mech. Eng. 99 (1992) 209-233.

[27] L.P. Franca and T.J.R. Hughes, Convergence analyses of Galerkin least–squares methods for symmetric advective–diffusive forms of the Stokes and incompressible Navier–Stokes equations, Comp. Meth. Appl. Mech. Eng. 105 (1993) 285-298.

[28] V. Girault, P.A. Raviart, Finite element methods for Navier-Stokes equations, (Springer, Berlin 1986).

[29] T.J.R. Hughes, Multiscale phenomena: Green's function, the Dirichet-to-Neumann formulation, subgrid scale models, bubbles and the origins of stabilized formulations, Comp. Meth. Appl. Mech. Eng. 127 (1995) 285-298.

[30] T.J.R. Hughes, G.R. Feijóo, L. Mazzei and J.B. Quincy, The variational multiscale method- a paradigm for computational mechanics, Comp. Meth. Appl. Mech. Eng. 166 (1998) 3-24.

[31] L.I.G. Kovasznay, Laminar flow behind a two-dimensional grid, Proc. Cambridge Philos. Soc. 44 (1948).

[32] G. Kunert, Robust a posteriori error estimation for a singularly perturbed reaction-diffusion equation on anisotropic tetrahedral meshes, Advances in Comp. Math. 15 (2001) 237-259.

[33] B. Jiang, T.L. Lin and L. A. Povinelli, Large-scale computation of incompressible viscous flow by least-squares finite element method, Comp. Meth. Appl. Mech. Eng. 114 (1994) 213-231.

[34] M.A. Maidana, M. Espino and J. Blasco, Un método estabilizado en elementos finitos 3D para el estudio de las corrientes oceánicas, Proceedings of the Congresso de Métodos Computacionais em Engenharia, Lisboa, Portugal (2004).

[35] S. Norburn and D. Silveser, Stabilized vs. stable mixed methods for incompressible flows, Comp. Meth. Appl. Mech. Eng. 166 (1998) 131-141.

[36] D. Silvester and N. Kechkar, Stabilized bilinear–constant velocity–pressure finite elements for the conjugate gradient solution of the Stokes problem, Comp. Meth. Appl. Mech. Eng. 79 (1990) 71-86.